

# Nanoscale

Accepted Manuscript



This is an *Accepted Manuscript*, which has been through the Royal Society of Chemistry peer review process and has been accepted for publication.

*Accepted Manuscripts* are published online shortly after acceptance, before technical editing, formatting and proof reading. Using this free service, authors can make their results available to the community, in citable form, before we publish the edited article. We will replace this *Accepted Manuscript* with the edited and formatted *Advance Article* as soon as it is available.

You can find more information about *Accepted Manuscripts* in the [Information for Authors](#).

Please note that technical editing may introduce minor changes to the text and/or graphics, which may alter content. The journal's standard [Terms & Conditions](#) and the [Ethical guidelines](#) still apply. In no event shall the Royal Society of Chemistry be held responsible for any errors or omissions in this *Accepted Manuscript* or any consequences arising from the use of any information it contains.

# Formation mechanism of bimetallic PtRu alloy nanoparticles in solvothermal synthesis†

Jian-Li Mi,<sup>\*a</sup> Peter Nørby,<sup>b</sup> Martin Bremholm,<sup>b</sup> Jacob Becker<sup>b</sup> and Bo B. Iversen<sup>\*b</sup>

<sup>a</sup>*Institute for Advanced Materials, School of Materials Science and Engineering, Jiangsu University, Zhenjiang 212013, China. Email: [jlmi@uj.edu.cn](mailto:jlmi@uj.edu.cn)*

<sup>b</sup>*Center for Materials Crystallography, Department of Chemistry and iNANO, Aarhus University, 8000 Aarhus C, Denmark. Email: [bo@chem.au.dk](mailto:bo@chem.au.dk)*

†Electronic Supplementary Information (ESI) available: Details of experiments, details of Rietveld refinements and refined parameters.

**Understanding the nucleation and growth mechanism of bimetallic nanoparticles in solvothermal synthesis is important for further development of nanoparticles with tailored nanostructure and properties. Here the formation of PtRu alloy nanoparticles in a solvothermal synthesis using metal acetylacetonate salts as precursors and ethanol as both solvent and reducing agent has been studied by *in situ* synchrotron radiation powder X-ray diffraction (SR-PXRD). Unlike the classical mechanism for the synthesis of monodispersed sols, the nucleation and growth processes of bimetallic PtRu nanoparticles occur simultaneously under solvothermal conditions. In the literature co-reduction of Pt and Ru is often assumed to be required to form PtRu bimetallic nanocrystals, but it is shown that monometallic Pt nanocrystals nucleate first and rapidly grow to an average size of 5 nm. Subsequently, the PtRu bimetallic alloy is formed in a second nucleation stage through a**

surface nucleation mechanism related to the reduction of Ru. The calculated average crystallite size of the resulting PtRu nanocrystals is smaller than that of the primary Pt nanocrystals due to the large disorder in the PtRu alloyed structure.

## Introduction

Bimetallic nanoparticles are of increasing importance in many areas related to green and sustainable energy applications, *e.g.* fuel cells, H<sub>2</sub> production and CO oxidation.<sup>1-3</sup> Control of composition, shape, particle size and architecture are critical factors in tailoring the catalytic properties of the bimetallic nanoparticles.<sup>4</sup> Establishing control over these factors requires a detailed understanding of the nucleation and growth mechanism of nanoparticles in solution.<sup>5</sup> In general, the nucleation and grain growth in the solid state have been studied in great detail, however, studies of kinetics under solvothermal conditions are still limited. Recently, there have been an increasing number of studies of nucleation mechanisms in solution thanks to the development of different *in situ* techniques. For example, with the use of *in situ* transmission electron microscopy, it has been suggested that the growth of Pt nanoparticles can take place either via monomer attachment or through particle coalescence.<sup>6</sup> *In situ* small-angle X-ray scattering and X-ray absorption near-edge spectroscopy have been applied to study the formation mechanism of gold nanoparticles,<sup>7</sup> and the nucleation kinetics of gold nanocrystals has been studied using *in situ* X-ray absorption fine structure spectroscopy.<sup>8</sup> While there has been significant progress in the understanding of the nucleation and growth of monometallic nanoparticles,<sup>6-8</sup> quantum dots,<sup>9</sup> metal oxides,<sup>10</sup> few studies have investigated the formation mechanism of bimetallic nanoparticles in solutions, especially, for solutions at high temperatures and high pressures. Although, many methods have been proposed for the synthesis of bimetallic

nanoparticles, it is highly challenging to synchronously control the nucleation and growth of bimetallic nanoparticles.<sup>11</sup> The particle architectures e.g. alloy, core-shell, or monometallic mixtures can be varied depending on the synthesis conditions. Generally, it is assumed that the alloyed bimetallic nanoparticles are formed by simultaneous reduction of the two corresponding two metal ions,<sup>12</sup> even though the thermodynamic and kinetic characteristics of the two distinct metals are always different. It is clearly of interest to study the exact formation mechanism during the reaction. The real-time probing of formation and growth is more complicated for bimetallic systems because the detailed structure and composition of the bimetallic nanoparticles are difficult to ascertain, especially during the reaction. An additional challenge for studies of the formation mechanisms under solvothermal conditions is the absorption and diffraction from the pressurized steel autoclaves or steel tubes. By using *in situ* synchrotron radiation powder X-ray diffraction (SR-PXRD) and specially designed sapphire capillary reactors, detailed information about the formation and growth has been achieved for different nanoparticles under solvothermal synthesis conditions.<sup>13</sup> In this communication, we report our studies of the formation mechanism of bimetallic PtRu alloy nanoparticles under solvothermal condition in real-time using the *in situ* SR-PXRD technique.

Previously we have developed a green solvothermal method for synthesis of metallic nanoparticles through the reduction of metal salts using solvents such as ethanol, *i.e.* without any strong or toxic reducing agents. As examples monometallic Pt and Ru nanoparticles have been prepared by using ethanol as both a solvent and a reducing agent.<sup>14,15</sup> Here, the solvothermal synthesis of PtRu nanoparticles from a mixture of ruthenium acetylacetonate ( $\text{Ru}(\text{acac})_3$ ) and platinum acetylacetonate ( $\text{Pt}(\text{acac})_2$ ) in ethanol solution has been carried out using a molar ratio of Pt:Ru = 1:1. A custom designed reactor that allows the real-time probing of SR-PXRD was used for the solvothermal synthesis.<sup>16</sup> The experiment was performed at a reaction temperature of

200 °C and a pressure of 25 MPa. Further experimental details are available in the supporting information.

## Results and Discussion

**Fig. 1a** shows the time evolution of the SR-PXRD patterns during the first 10 min of the solvothermal synthesis of PtRu nanoparticles. Before heating, diffraction peaks from the precursor are observed, because the precursor is not fully dissolved. As shown in **Fig. 1b**, no diffraction peaks are observed in the diffraction pattern at a reaction time of 5 s, which shows that the precursor is fully dissolved before any nucleation is observed. After a reaction time of 10 s diffraction peaks corresponding to a face-centered cubic (fcc) structure are observed with unit cell parameters that match monometallic Pt. The integrated intensity of the diffraction peaks increase with reaction time and become sharper at 15 s, but then broaden again with further reaction at 2 and 10 min. No diffraction peaks from other phases are observed. The positions of the diffraction peaks at 2 and 10 min shift to higher angles compared with those at 10 and 15 s, indicating that the composition of the nanoparticles changes during the reaction.

In order to obtain more detailed microstructural information, the *in situ* SR-PXRD data were corrected for instrumental broadening using a LaB<sub>6</sub> standard and analyzed by Rietveld refinement using the FullProf program.<sup>17</sup> Besides the scale factor and the unit cell parameter, a Lorentzian peak-shape parameter is refined and the crystallite size is calculated from the peak-shape parameter.<sup>18</sup> The refined SR-PXRD patterns for PtRu nanoparticles show good agreement with the observed patterns (**Fig. S1**). Selected refinement parameters are displayed in **Table S1** for the *in situ* PXRD patterns at the reaction time of 10 s, 15 s, 2 min and 10 min, respectively. The relation between the composition and the cell parameter of Pt-Ru alloys with fcc structure has

been studied in great detail and it is well established that PtRu is contracted compared with that of pure Pt.<sup>19</sup> In the present study, cell parameters of 3.9304(2) and 3.9312(2) Å are obtained for particles at reaction time of 10 and 15 s, respectively, which are quite close to that of monometallic Pt of 3.924 Å.<sup>20</sup> On the other hand cell parameters of 3.8978(2) and 3.9084(2) Å are obtained for particles at reaction time of 2 and 10 min, respectively, which are comparable to that of PtRu alloy with the cell parameter of 3.889 Å.<sup>1</sup> Although a direct comparison of the unit cell parameters from different studies requires some caution because of potential systematic errors (e.g. different setup, different crystallite sizes and temperature), then the *in situ* data are collected at the exact same reaction conditions in a single experiment, and this ensures good correspondence between the data points and clearly shows the relative change of unit cell parameters with reaction time. There is a general understanding that co-reduction of the two metals ions is required to form bimetallic alloy nanoparticles,<sup>11,12</sup> but this suggestion has never been fully supported due to lack of knowledge about whether the two metals ions are really reduced simultaneously. The fact that reduction of Pt is observed to precede that of Ru under the present solvothermal conditions can be understood since Pt is a more noble metal than Ru.<sup>21</sup> Compared to the particles at 15 s, the particles at 2 and 10 min show broader diffraction peaks. Bimetallic alloyed nanoparticles have a random distribution of the two elements, resulting in large disorder and strain in the crystal structure. It has been verified in many studies that the average diameters calculated from PXRD data are lower than the diameters determined by TEM measurements for alloyed nanoparticles.<sup>22</sup> It has furthermore been shown that bimetallic alloyed PtRu nanoparticles have broader X-ray diffraction peaks than Pt nanoparticles with similar particle sizes.<sup>23</sup> As a result, the broader diffraction peaks for the particles at 2 and 10 min suggest that the nanoparticles are less ordered, indicating a formation of bimetallic alloyed nanoparticles.

Thus, bimetallic PtRu alloyed nanoparticles in the present study are formed through a second stage of nucleation and growth rather than by co-reduction of Pt and Ru ions from the solution.

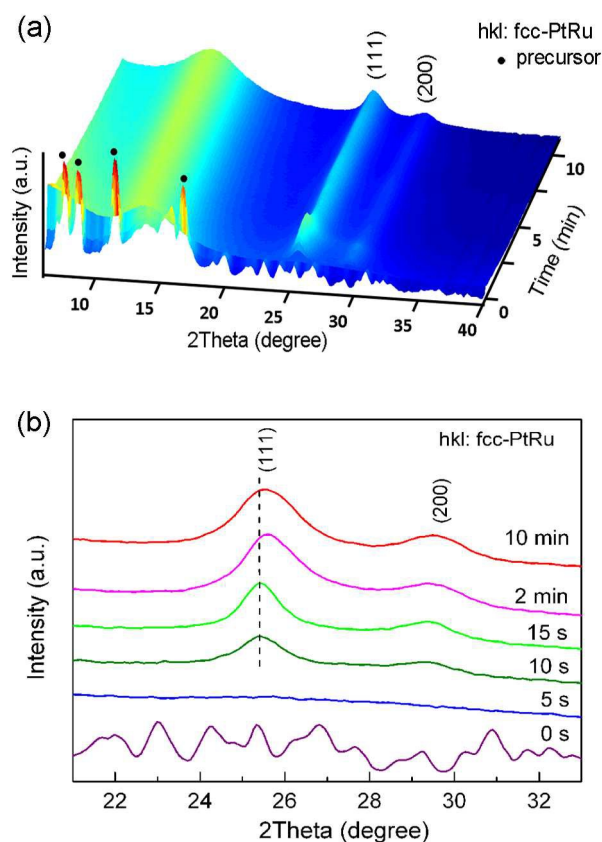


**Fig. 1** (a) Time resolved *in situ* SR-PXRD patterns showing the transformation of the precursor to bimetallic PtRu alloy nanoparticles. (b) PXRD patterns at selected reaction time of 0 s, 5 s, 10 s, 15 s, 2 min and 10 min. The dashed line marks the Bragg angle for the primary nanoparticles.

For a detailed understanding of the nucleation mechanism and growth kinetics of PtRu nanoparticles, the refined scale factors, crystallite sizes and unit cell parameters are plotted as functions of reaction time as in **Fig. 2**. The relative amount of the product can be estimated from the scale factors. It can be seen that the scale factor (normalized to the equilibrium value) increases with reaction time and reaches a maximum after 2 min indicating that the formation of

the PtRu nanoparticles occurs in only about 2 min. The nucleation and growth of particles under solvothermal conditions is usually different from the formation of monodispersed sols from solutions at ambient pressure or from the crystallization in solid state reactions. The classical nucleation and growth mechanism of monodisperse sols was first explained by LaMer and requires separation of nucleation and growth into two stages.<sup>24</sup> The formation of bimetallic PtRu in the present study clearly proceeds via a very different route. The Avrami equation<sup>25</sup> is often used to describe the kinetics of crystallization for solid-state transformations. Here we attempt to use the Avrami equation to describe the formation process of bimetallic PtRu under solvothermal condition, even though it is not the same as a solid-state phase transformation:

$$\alpha = 1 - \exp [-(kt)^n] \quad (1)$$

where  $k$  is a rate constant related to the activation energy,  $\alpha$  is the fraction of transformation,  $t$  is the reaction time and  $n$  is a parameter related to the crystallization mechanisms.<sup>26</sup> Bulk nucleation mechanisms often result in  $n$  parameters larger than 1 and surface nucleation yields  $n \sim 1$ .<sup>27,28</sup>  $\alpha$  is estimated from the normalized scale factors. It is found that the time evolution of the scale factor fits the Avrami equation quite well with the fitting values of  $k = 2.5(1) \text{ min}^{-1}$  and  $n = 1.1(1)$ . This suggests that the formation of PtRu is mainly via a surface nucleation mechanism. This can be interpreted as initial fast formation of monometallic Pt nanoparticles, followed by the second stage of relative slower nucleation of PtRu nanoparticles on the surface of the primary Pt nanoparticles. However, more evidence is needed to clarify whether the present non solid-state transformation obeys the Avrami equation. The mechanism could also be described as a two-step mechanism for transition-metal nanocluster formation, including nucleation ( $A \rightarrow B$ , rate constant  $k_1$ ) and autocatalytic growth ( $A + B \rightarrow 2B$ , rate constant  $k_2$ ), in which A represents the precursor and B represents the growing nanocluster.<sup>29,30</sup> The rate constant  $k_1$  is inversely

proportional to the length of the induction period and  $k_2$  is proportional to the normalized slope of the linear part of the curve after the induction period. As shown in **Fig. S2**, a reasonable fit of the kinetic curve with  $k_1 = 2.2(5) \text{ min}^{-1}$  and  $k_2 = 0.7(2) \text{ min}^{-1}$  is obtained for the two-step mechanism.

As shown in **Fig. 2a**, the crystallite size increases rapidly in the beginning and reaches a maximum value of 4.9 nm at a reaction time of 10 s showing the nucleation and growth of Pt nanoparticles. Afterwards, the crystallite size decreases with reaction time to an equilibrium value of ~3 nm at 2 min illustrating the formation and alloying process of PtRu nanoparticles. It should be noted that the crystallite size determined by PXRD in this case is not the real particle size. The real particle size of PtRu particles should increase compared to primary Pt particles due to the growth of the nanoparticles. The calculated crystallite size of PtRu is smaller than Pt, and this is explained by the larger disorder in the bimetallic crystal structure due to the random distribution of the two elements. Accordingly, the unit cell parameter decreases from that of pure Pt to bimetallic PtRu as shown in **Figure 2b**. The slight increase of unit cell parameter during the reaction from 2 to 5 min could be due to the composition homogenization of the PtRu nanoparticles. It could also be attributed to an increase of particle sizes which results in a decrease of surface stress, though it is not revealed by the crystallite size curve.

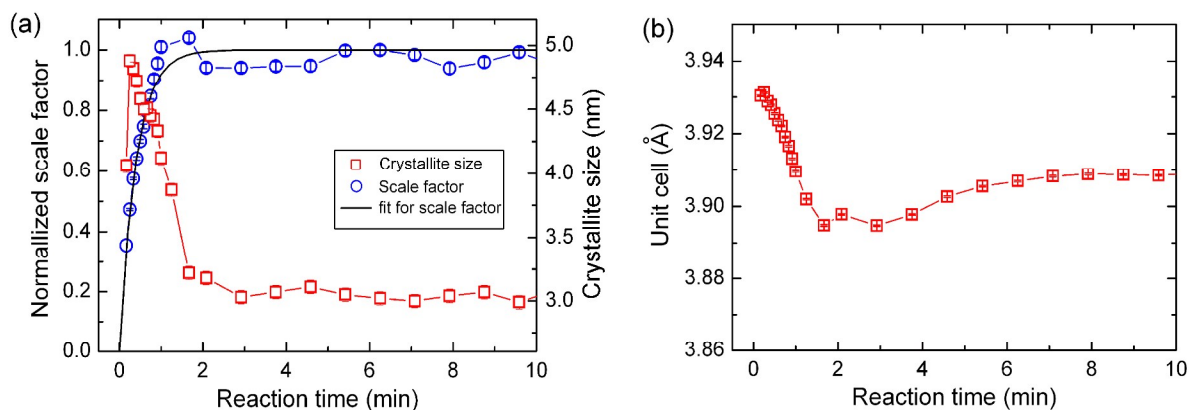


**Fig. 2** (a) Time evolution of normalized scale factor and crystallite size of products. The normalized scale factor represents the formation curve during the reaction and the solid line is a fit using Avrami equation to the formation curve. (b) Time evolution of unit cell parameter of the products.

On the basis of the above analysis, a formation mechanism of PtRu nanoparticles can be proposed under solvothermal conditions using metal acetylacetonate salts as precursors and ethanol as both solvent and reducing agent as shown in **Fig. 3**. Initially, the metal salt precursors are dissolved in ethanol (**Fig. 3a**). Next, the nucleation of Pt occurs very quickly and rapid growth of the Pt nanoparticles occurs simultaneously (**Fig. 3b**). At a reaction time of 20 s, a second stage of nucleation occurs due to the slower reduction of Ru and surface nucleation occurs on the primary Pt nanoparticles (**Fig. 3c**). Finally, PtRu alloyed bimetallic nanoparticles are formed by a diffusion process (**Fig. 3d**). In some *ex situ* TEM studies of Pt-based alloy nanoparticles it was also suggested that the formation of bimetallic alloy nanoparticles does not take place via simultaneous co-reduction, for example, the nucleation of Pt occurs firstly for PtRu nanoparticles,<sup>31</sup> while the nucleation of Pd is observed to precede that of Pt for PtPd nanocrystals.<sup>32</sup>

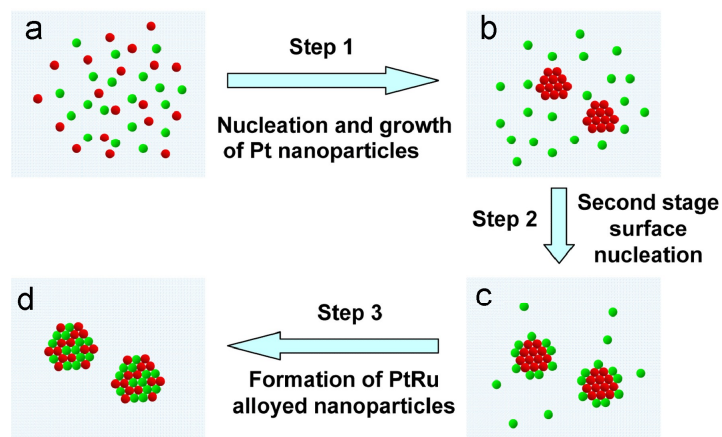


**Fig. 3** Schematic illustration of the formation mechanism of PtRu nanoparticles.

## Conclusions

By using *in situ* SR-PXRD, we have studied the nucleation and growth mechanism of bimetallic PtRu alloy nanoparticles during the solvothermal synthesis process. The analysis of *in situ* SR-PXRD indicates it only takes about 2 min for the formation of PtRu nanoparticles. Contrary to general expectation the nanoparticle formation does not take place via simultaneous co-reduction of the metal salts. Instead the formation mechanism of PtRu involves several steps. Initially, Pt nucleates and grows very quickly. Subsequently, Ru atoms are reduced and deposited to the primary Pt nanoparticles. Finally, Ru atoms diffuse to the nanoparticles and PtRu alloyed nanoparticles are formed. The random distribution of the two elements results a strain-broadening in the diffraction patterns of PtRu alloyed nanoparticles. Due to the large disorder in the PtRu alloyed structure, the calculated crystallite size of PtRu nanoparticles is smaller than the primary Pt nanoparticles, despite of the growth of nanoparticles. These findings enrich our

understanding of the nucleation process of the formation of bimetallic nanoparticles formation under solvothermal condition.

## Acknowledgements

This work was supported by National Natural Science Foundation of China (Grant 51401089), the Natural Science Foundation of Jiangsu Province (Grant BK20140552), the Scientific Research Foundation of Jiangsu University (Grant 14JDG013), the Danish National Research Foundation (Center for Materials Crystallography, DNRF93), the Danish Innovation Foundation (FuelScaleIntegrate), and the Danish Research Council for Nature and Universe (DanScatt). The authors are grateful for the beamtime obtained at the beamline I711, MAX-lab synchrotron radiation source, Lund University, Sweden.

## References

- 1 S. Alayoglu, A. U. Nilekar, M. Mavrikakis and B. Eichhorn, *Nat. Mater.*, 2008, **7**, 333-338.
- 2 G. W. Huber, J. W. Shabaker and J. A. Dumesic, *Science*, 2003, **300**, 2075-2077.
- 3 F. Maroun, F. Ozanam, O. M. Magnussen and R. J. Behm, *Science*, 2001, **293**, 1811-1814.
- 4 S. Alayoglu, P. Zavalij, B. Eichhorn, Q. Wang, A. I. Frenkel and P. Chupas, *ACS Nano*, 2009, **3**, 3127-3137.
- 5 Y. Wu, D. Wang and Y. Li, *Chem. Soc. Rev.*, 2014, **43**, 2112-2124.
- 6 H. Zheng, R. K. Smith, Y. Jun, C. Kisielowski, U. Dahmen and A. P. Alivisatos, *Science*, 2009, **324**, 1309-1312.
- 7 J. Polte, T. Ahner, F. Delissen, S. Sokolov, F. Emmerling, A. F. Thünemann and R. Kraehnert, *J. Am. Chem. Soc.*, 2010, **132**, 1296-1301.
- 8 T. Yao, Z. Sun, Y. Li, Z. Pan, H. Wei, Y. Xie, M. Nomura, Y. Niwa, W. Yan, Z. Wu, Y. Jiang, Q. Liu and S. Wei, *J. Am. Chem. Soc.*, 2010, **132**, 7696-7701.

- 9 B. Abécassis, C. Bouet, C. Garnero, D. Constantin, N. Lequeux, S. Ithurria, B. Dubertret, B. R. Pauw and D. Pontoni, *Nano Lett.*, 2015, **15**, 2620-2626.
- 10 N. T. K. Thanh, N. Maclean and S. Mahiddine, *Chem. Rev.*, 2014, **114**, 7610-7630.
- 11 A. D. Banadaki and A. Kajbafvala, *J. Nanomater.*, 2014, **2014**, 985948.
- 12 N. Toshima and T. Yonezawa, *New J. Chem.*, 1998, **22**, 1179-1201.
- 13 K. M. Ø. Jensen, C. Tyrsted, M. Bremholm and B. B. Iversen, *ChemSusChem*, 2014, **7**, 1594-1611.
- 14 J. L. Mi, H. F. Clausen, M. Bremholm, M. S. Schmøkel, P. Hernández-Fernández, J. Becker and B. B. Iversen, *Chem. Mater.*, 2015, **27**, 450-456.
- 15 J. L. Mi, Y. Shen, J. Becker, M. Bremholm and B. B. Iversen, *J. Phys. Chem. C*, 2014, **118**, 11104-11110.
- 16 J. Becker, M. Bremholm, C. Tyrsted, B. Pauw, K. M. Ø. Jensen, J. Eltzholt, M. Christensen and B. B. Iversen, *J. Appl. Cryst.*, 2010, **43**, 729-736.
- 17 J. Rodriguez-Carvajal, *Physica B*, 1993, **192**, 55-69.
- 18 M. Bremholm, J. Becker-Christensen and B. B. Iversen, *Adv. Mater.*, 2009, **21**, 3572-3575.
- 19 Z. Liu, E. T. Ada, M. Shamsuzzoha, G. B. Thompson and D. E. Nikles, *Chem. Mater.*, 2006, **18**, 4946-4951.
- 20 J. W. Edwards, R. Speiser and H. L. Johnston, *J. Appl. Phys.*, 1951, **22**, 424-428.
- 21 W. E. Mustain, H. Kim, V. Narayanan, T. Osborn and P. A. Kohl, *J. Fuel Cell Sci Tech*, 2010, **7**, 041013.
- 22 X. Wang, L. Altmann, J. Stöver, V. Zielasek, M. Bäumer, K. Al-Shamery, H. Borchert, J. Parisi and J. Kolny-Olesiak, *Chem. Mater.*, 2013, **25**, 1400-1407.
- 23 C. Nethravathi, E. A. Anumol, M. Rajamathi and N. Ravishankar, *Nanoscale.*, 2011, **3**, 569-571.
- 24 V. K. LaMer and R. H. Dinegar, *J. Am. Chem. Soc.*, 1950, **72**, 4847-4854.
- 25 M. Avrami, *J. Phys. Chem.*, 1939, **7**, 1103-1112.
- 26 H. Zhang and J. F. Banfield, *Chem. Mater.*, 2002, **14**, 4145-4154.
- 27 K. Matusita and S. Sakka, *J. Non-Cryst. Solids*, 1980, **38**, 741-746.
- 28 M. Fernández-García, X. Wang, C. Belver, J. C. Hanson and J. A. Rodriguez, *J. Phys. Chem. C*, 2007, **111**, 674-682.
- 29 M. A. Watzky and R. G. Finke, *J. Am. Chem. Soc.* 1997, **119**, 10382-10400.

- 30 M. A. Watzky, E. E. Finney and R. G. Finke, *J. Am. Chem. Soc.* 2008, **130**, 11959-11969.
- 31 Y. Lu and W. Chen, *Chem. Commun.*, 2011, **47**, 2541-2543.
- 32 Y. Lu, Y. Jiang and W. Chen, *Nanoscale* 2014, **6**, 3309-3315.

## Table of Contents (TOC) Image

